

- Thomas, *Faraday Discuss. R. Soc. Chem.* **105**, 1 (1996); *Chem. Eur. J.* **3**, 1557 (1997).
14. B. F. G. Johnson *et al.*, *J. Organomet. Chem.* **191**, C3 (1980); P. J. Bailey *et al.*, *J. Chem. Soc. Dalton Trans.* **1996**, 3515 (1996).
 15. J. M. Thomas, E. L. Evans, J. O. Williams, *Proc. R. Soc. London Ser. A* **331**, 417 (1972); G. M. Francis, I. M. Goldby, L. Kuipers, B. Vonissendorff, R. E. Palmer, *J. Chem. Soc. Dalton Trans.* **1996**, 665 (1996).
 16. O. P. Bahl, E. L. Evans, J. M. Thomas, *Surf. Sci.* **8**, 473 (1967).
 17. J. Sloan, J. Cook, M. L. H. Green, J. L. Hutchison, R. Tenne, *J. Mater. Chem.* **7**, 1089 (1997).
 18. All reactions were carried out under exclusion of air using solvents freshly distilled under an atmosphere of nitrogen. IR spectra were recorded on a Perkin-Elmer 1600 series Fourier transform IR spectrometer in CH₂Cl₂ using NaCl cells or a Nujol mull. Negative fast ion bombardment mass spectra were obtained using a Kratos MS50TC spectrometer, with Csl as calibrant. Separation of products was accomplished with Merck thin layer chromatography plates as supplied (0.25-mm layer of Kieselgel 60 F254). [Ru₆C(CO)₁₆][PPN]₂, [H₂Ru₁₀(CO)₂₅][PPN]₂, and MCM-41 were prepared by literature procedures (14).
 19. Ether and CH₂Cl₂ were found to be the most effective of several combinations. The small amount of CH₂Cl₂ is thought to ferry the cluster salt through the liquid phase to the silica surface; upon contact with the surface, the (predominantly) CH₂Cl₂ solvation shell is substituted by the silanol groups. The solvent molecules enable repetition of this cycle: Entropy change provides the driving force for the anions to enter the mesopores by way of substituting for loosely held solvent molecules, whereas the drop in enthalpy directs the ordering of the sorbed clusters onto the pore walls.
 20. MCM-41 powder (200 mg) was dried under high vacuum (0.01 mm Hg) at 473 K for 6 hours. This was then slurried with dry ether (30 ml) and I or II along with CH₂Cl₂ (0.1 ml) at ambient temperature in the absence of light for 72 hours. The resulting red or brown solid was washed with ether (10 ml) and dried under high vacuum (0.01 mm Hg). Spectroscopic data for MCM-41-Ru₆: IR (Nujol): ν (CO) 2056 (w), 1968 (vs), 1929 (m, sh), 1910 (m), 1816 (w, sh), 1795 (w), 1727 (s) cm⁻¹. Spectroscopic data for MCM-41-Ru₁₀: IR (Nujol): ν (CO) 2053 (m), 2044 (w, sh), 2007 (vs), 1989 (s, sh), 1955 (s, sh), 1931 (s), 1780 (w), 1751 (w), 1709 (w) cm⁻¹ (w, weak; m, medium; s, strong; vs, very strong; sh, shoulder).
 21. Similar experiments at the Synchrotron Source (Daresbury Lab, UK) will soon be carried out on MCM-41, I and II (D. S. Shephard and G. Sankar, in preparation).
 22. D. A. Jefferson *et al.*, *Nature* **323**, 428 (1986); G. R. Millward and J. M. Thomas, in *Proceedings of Carbon and Graphite Conference* (Society of Chemical Industry, London, 1974), pp. 492–497.
 23. HRTEM images were recorded with a JEOL JEM-200CX electron microscope operating at 200 kV with a modified specimen stage with objective lens parameters C_s = 0.41 mm and C_c = 0.95 mm, giving an interpretable point resolution of ~0.185 nm. STEM experiments were conducted using a field emission dedicated microscope (VG HB501). MCM-41 samples were prepared by crushing the particles between two glass slides and spreading them on a holey carbon film supported on a Cu grid. The samples were briefly heated under a tungsten filament light bulb in air before transfer into the specimen chamber. The images were recorded at magnifications of 24,000× to 49,000×.
 24. Although STEM images display less contrast than the corresponding HRTEM images, STEM enables shorter exposure times, hence electron-beam damage is reduced.
 25. D. A. Jefferson *et al.*, *Nature* **281**, 51 (1979).
 26. The hexagonal MCM-41 model with a framework based on silica glass structures was modeled by molecular dynamics [B. Vessal, M. Amini, D. Fincham, *J. Non-Cryst. Solids* **159**, 184 (1993)]. The channel volume was excised from the glass structure, and the resulting dangling bonds were satisfied by H (to O) or by OH (to Si). The unit cell parameters are a = 3.703 nm and c = 7.98 nm. The pore wall thickness is ~0.6 nm. The resulting periodic structure was optimized by energy minimization with the program Discover [version 4.0.0; Molecular Simulations Inc., San Diego, CA (1996)] with the cff91_czeo force field [J. R. Hill and J. Sauer, *J. Phys. Chem.* **98**, 1238 (1994)] and later with the program GULP [General Utility Lattice Program; J. D. Gale, Royal Institution and Imperial College, London (1991)]. Three clusters of [H₂Ru₁₀(CO)₂₅][PPN]₂ were loaded with an intercluster distance of 2.66 nm.
 27. For hydrogenation of hex-1-ene, a 150-ml Teflon-lined autoclave equipped with a magnetic follower was charged with 8.2 mg of MCM-41-Ru₁₀, 3.0 ml of hex-1-ene, and H₂ at 65 atm. After heating to 393 K for 4 hours, the vessel was cooled to ambient temperature and the contents analyzed by ¹H NMR to reveal >99% conversion to n-hexane. A subsequent run was performed with 12 ml of hex-1-ene to establish the turnover frequency (TOF). This gave 15% conversion to hex-2-ene and 50% conversion to hexane, yielding a TOF of 4400-mol[Hex]/mol[Ru₁₀]⁻¹ hour⁻¹. For hydrogenation of cis-cyclooctene, a 250-ml Erlenmeyer flask equipped with a magnetic follower was charged with ~10 mg of MCM-41-Ru₆, 10 ml of cis-cyclooctene, and H₂ at 1 atm. The flask was kept at 298 K for 72 hours, during which time the contents were analyzed by ¹H NMR and gas chromatography-mass spectrometry. The analysis showed a steady conversion to cyclooctane; no unconverted starting material was detected after 72 hours. From these results, an overall TOF of ~130 mol[Cyclo-C₈]/mol[Ru₆]⁻¹ hour⁻¹ was calculated.
 28. M. E. Raimondi, T. Maschmeyer, R. H. Templer, J. M. Seddon, *J. Chem. Soc. Chem. Commun.* **1997**, 1843 (1997).
 29. T. R. Felthouse *et al.*, in *Advanced Catalysts and Nanostructured Materials: Modern Synthetic Methods*, W. R. Mozar, Ed. (Academic Press, San Diego, CA, 1996), pp. 91–115.
 30. Supported by an Engineering and Physical Sciences Research Council (UK) rolling grant (J.M.T.), post-doctoral research award (B.F.G.J.), a European Union (EU) TMR award (B.F.G.J.), an EU Fellowship TMR (T.M.), the University of Cambridge, and the Royal Society for the Smithson Research Fellowship (Peterhouse) (D.S.S.). W.Z. thanks D. A. Jefferson for many helpful discussions.

6 January 1998; accepted 5 March 1998

A Trivalent System from Vancomycin·D-Ala-D-Ala with Higher Affinity Than Avidin·Biotin

Jianghong Rao, Joydeep Lahiri, Lyle Isaacs, Robert M. Weis, George M. Whitesides*

Tris(vancomycin carboxamide) binds a trivalent ligand derived from D-Ala-D-Ala with very high affinity: dissociation constant (K_d) $\approx 4 \times 10^{-17} \pm 1 \times 10^{-17}$ M. High-affinity trivalent binding and monovalent binding are fundamentally different. In trivalent (and more generally, polyvalent) binding, dissociation occurs in stages, and its rate can be accelerated by monovalent ligand at sufficiently high concentrations. In monovalent binding, dissociation is determined solely by the rate constant for dissociation and cannot be accelerated by added monomer. Calorimetric measurements for the trivalent system indicate an approximately additive gain in enthalpy relative to the corresponding monomers. This system is one of the most stable organic receptor-ligand pairs involving small molecules that is known. It illustrates the practicality of designing very high-affinity systems based on polyvalency.

Polyvalent inhibitors can be used for blocking the adhesion of pathogens to the surfaces of target cells (1, 2). The enhanced biological activity observed in these systems has been rationalized in terms of the roles of enthalpy and entropy. Similar strategies using polyvalency may also be applied to other problems in biochemistry such as blocking carbohydrate-protein interactions and controlling cellular signal transduction (3–7). We describe the design and synthesis of a trivalent system of receptor and ligand derived from vancomycin and D-Ala-D-Ala (DADA), respectively, that shows exceptionally high affinity [its binding constant

(K_d) is $\sim 4 \times 10^{-17} \pm 1 \times 10^{-17}$ M, 25 times tighter than biotin·avidin, which is one of the strongest interactions known in biological systems (8)] and we characterize the thermodynamics and kinetics of this high-affinity system.

We chose the vancomycin·DADA pair for elaboration into a polyvalent system for five reasons: (i) vancomycin is relatively rigid, and there is little loss in conformational entropy on binding (Table 1) (9); (ii) Williams and others have studied it in detail structurally (10–12) and thermodynamically (9, 13); (iii) the two components are readily available and relatively easily modified synthetically (7); (iv) the monovalent complex has a convenient binding constant ($K_d \approx 1 \mu\text{M}$) (14); and (v) Williams proposed that noncovalent divalency is important in the binding of vancomycin to DADA groups in bacterial cell walls (15–17).

The design of the trivalent vancomycin

J. Rao, J. Lahiri, L. Isaacs, G. M. Whitesides, Department of Chemistry and Chemical Biology, Harvard University, 12 Oxford Street, Cambridge, MA 02138, USA.
R. M. Weis, Department of Chemistry, University of Massachusetts, Amherst, MA 01003, USA.

*To whom correspondence should be addressed. E-mail: gw Whitesides@gmwhgroup.harvard.edu

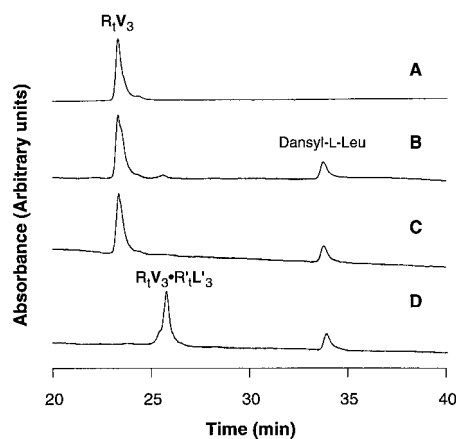
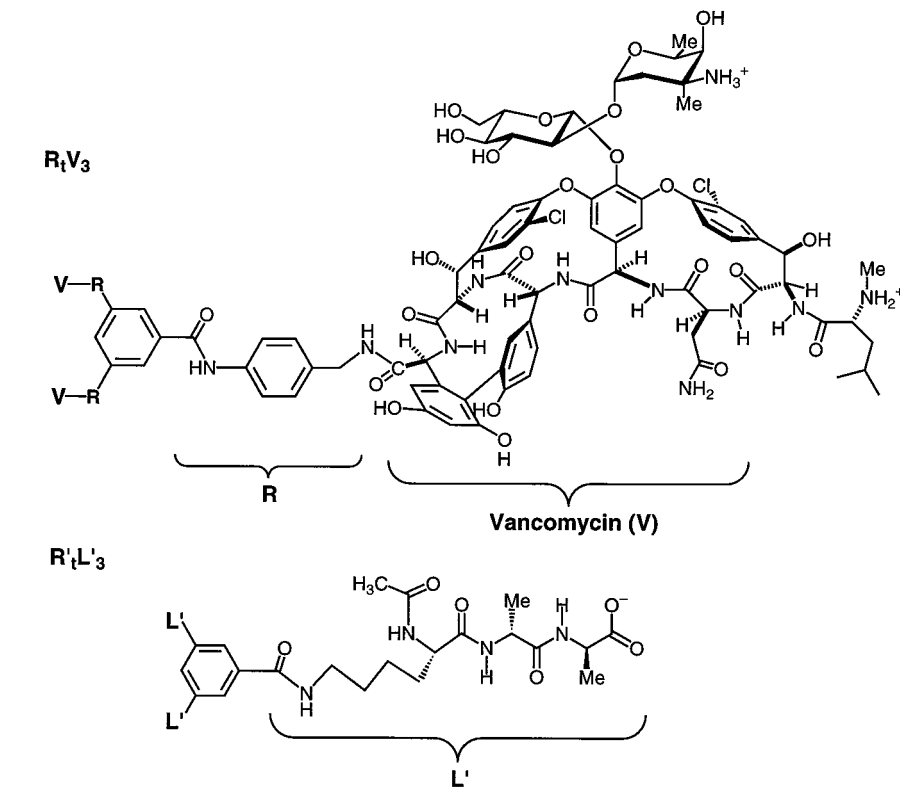


Fig. 1. HPLC of aliquots of samples that contained (A) R_tV_3 (4.5 μ M); (B) R_tV_3 (4.5 μ M); (C) R_tV_3 (4.5 μ M) + **L** (19.1 mM); and (D) R_tV_3 (4.5 μ M) + $R'_tL'_3$ (4.5 μ M). Dansyl-L-Leu (10 μ M) was introduced into each sample except (A) as an internal standard. All analyses were carried out under the same conditions, with a Rainin (Woburn, Massachusetts) analytical reverse-phase C18 column, linear eluting gradient from 85% solvent A [0.1% trifluoroacetic acid (TFA) in water] and 15% solvent B (0.1% TFA in acetonitrile) to 70% A and 30% B, over 45 min. The absorbance was monitored at 280 nm wavelength.

derivative R_tV_3 [$C_6H_3-1,3,5-(CONHC_6H_4-4-CH_2NHC(O)V)_3$; **V** = Vancomycin] and the trivalent derivative of DADA, $R'_tL'_3$ [$C_6H_3-1,3,5-(CON^eH(N^a\text{-acetyl})-L\text{-Lys-D-Ala-D-Ala})_3$], was based on the geometry of the monovalent complex (18) and on the positions available for modification (Scheme 1) (19). The central aromatic spacer was designed to be large enough to accommodate three vancomycin molecules and rigid to minimize the loss of conformational entropy on binding. Syntheses were modeled on literature precedents (7, 19); 1H nuclear magnetic resonance (NMR) spectra and electrospray ionization mass spectrometry (ESIMS) confirmed the structures (20).

We examined the stability of the complex $R_tV_3 \cdot R'_tL'_3$ by high-pressure liquid chromatography (HPLC). On injecting a mixture of R_tV_3 and $R'_tL'_3$, we observed only the aggregate $R_tV_3 \cdot R'_tL'_3$; we did not observe free R_tV_3 ($R_tV_3 \cdot R'_tL'_3$ and R_tV_3 have clearly distinguishable retention times) (Fig. 1D). In a control experiment, we examined a mixture of R_tV_3 (4.5 μ M) and a monovalent ligand **L**, diacetyl-L-Lys-D-Ala-D-Ala (19.1 mM), by HPLC under otherwise identical conditions; this experiment showed only the presence of R_tV_3 (Fig. 1C). We inferred that the 1:3 complex of $R_tV_3 \cdot 3L$ that was undoubtedly present at equilibrium dissociated completely during the passage through the column; the fact that the peak for R_tV_3 was sharp indicated that dissociation was fast



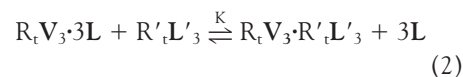
Scheme 1. Structures of the trivalent derivatives of vancomycin, R_tV_3 , and of DADA, $R'_tL'_3$.

under the conditions of the experiment (21). We concluded that $R_tV_3 \cdot R'_tL'_3$ was stable enough to survive the HPLC experiments intact. Therefore, we used HPLC to quantitate the relative amounts of $R'_tL'_3$, R_tV_3 , and $R_tV_3 \cdot R'_tL'_3$ in a mixture of these species and to estimate the trivalent dissociation constant K_d^t (Eq. 1). A direct titration of R_tV_3 with $R'_tL'_3$, however, was not



successful; the reaction was stoichiometric even when R_tV_3 was at its minimum de-

tectable concentration [in the micromolar range for the ultraviolet (UV) detector]. Thus, we turned to a competition assay to estimate K_d^t indirectly from the equilibrium constant K (Eqs. 2 and 3);



$$K = \frac{[R_tV_3 \cdot R'_tL'_3][L]^3}{[R_tV_3 \cdot 3L][R'_tL'_3]} = \frac{(K_d^m)^3}{K_d^t} \quad (3)$$

here, K_d^m is the average monovalent dissociation constant of the complex $R_tV_3 \cdot 3L$

Table 1. Thermodynamic parameters of binding of derivatives of vancomycin to derivatives of DADA at 298 K. Values of ΔH° were determined by duplicated ITC titrations at pH 7.0 in 5.0 mM phosphate buffer at 298 K; values for the free energy ΔG° were calculated from K_d , measured in the same solution except for that of $R_tV_3 \cdot R'_tL'_3$; values of $-T\Delta S^\circ$ were calculated from $\Delta G^\circ = \Delta H^\circ - T\Delta S^\circ$. In the cases of 1:3 or 3:1 complexes, the three binding sites were treated as independent in the analyses. Errors are estimated as 25% for K_d and 5% for ΔH° . $R'_tL'_3$ and **RV** are the monovalent derivatives of DADA and **V**, N^a -acetyl- N^e -benzoyl-L-Lys-D-Ala-D-Ala; **RV**, $C_6H_5CONHC_6H_4-4-CH_2NHC(O)V$.

Receptor	Ligand	Receptor/ ligand	K_d (M)	ΔG° (kJ/mol)	ΔH° (kJ/mol)	$-T\Delta S^\circ$ (kJ/mol)
R_tV_3	$R'_tL'_3$	1:1	$4 \times 10^{-17} \pm 1 \times 10^{-17}$	-94	-167	73
Vancomycin*	L	1:1	1.6×10^{-6}	-33.0	-50.2	17.2
R_tV_3	R'_tL'	1:3	1.1×10^{-6}	-33.9	-51.9	18.0
R_tV_3	L	1:3	2.7×10^{-6}	-31.8	-50.2	18.4
Vancomycin	$R'_tL'_3$	3:1	0.34×10^{-6}	-36.8	-73.2	36.4
RV	$R'_tL'_3$	3:1	0.11×10^{-6}	-39.7	-74.1	34.4
RV	R'_tL'	1:1	0.96×10^{-6}	-34.3	-87.9	53.6

*Measured in 20 mM phosphate buffer at 298 K; the results agree well with the literature values (13).

and was estimated as 5 μM by UV difference spectroscopy (14, 22).

We allowed $R'_tL'_3$ to compete with the monovalent ligand L for R_tV_3 ; the concentration of L used in the assay was chosen such that at least 99% of the three vancomycin binding sites on R_tV_3 were saturated, and that on addition of $R'_tL'_3$, there was a quantifiable concentration of free $R'_tL'_3$ in solution at equilibrium in the system. We defined θ as a measure of the progress of the exchange reaction on addition of $R'_tL'_3$ (Eq. 4); θ is the fraction of total R_tV_3 present in the sample that is in the form of $R_tV_3 \cdot R'_tL'_3$.

$$\theta = \frac{[R_tV_3 \cdot R'_tL'_3]}{[R_tV_3 \cdot 3L] + [R_tV_3 \cdot R'_tL'_3]} \quad (4)$$

$$\frac{\theta}{[R'_tL'_3]} = -\frac{K}{[L]^3} \theta + \frac{K}{[L]^3} \quad (5)$$

Equation 5, obtained by combination of Eqs. 3 and 4, was used to characterize the binding (23): if the ratios of $\theta/[R'_tL'_3]$ are plotted versus θ , a straight line would be expected; both the slope and y intercept of this line would afford the ratio of $K/[L]^3$ and thus the value of K . The values of θ and $[R'_tL'_3]$ were determined from the HPLC titrations (24). The ratios of $\theta/[R'_tL'_3]$ were then plotted versus θ . As expected, the plot gave a straight line and yielded the value of K (Fig. 2). We estimated K_d^t using K_d^m and K (Eq. 3); our estimate of K_d^t is $\sim 4 \times 10^{-17} \pm 1 \times 10^{-17}$ M. This dissociation constant is lower than that of biotin:avidin ($K_d \approx 10^{-15}$ M) (8).

At first, the conclusion that R_tV_3 bound very tightly to $R'_tL'_3$ seemed at odds with the relatively fast equilibrium we observed in solutions containing R_tV_3 , $R'_tL'_3$, and L . If we assume that the rate constant for association of R_tV_3 and $R'_tL'_3$, k_{on} , is approximately nine times that for association

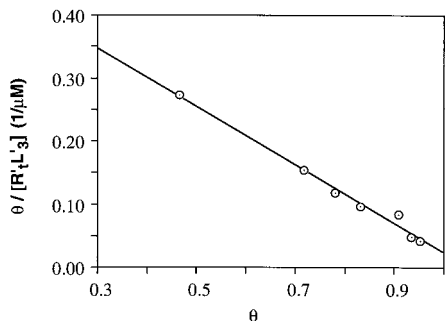


Fig. 2. A plot of the ratios of $\theta/[R'_tL'_3]$ versus θ for the titration of R_tV_3 (4.5 μM) with $R'_tL'_3$ (0 to 35 μM) in the presence of L (19.1 mM). The line is a linear fit of the data to Eq. 5. The slope of the line yields a value of $K/[L]^3 \approx 0.47 \mu\text{M}^{-1}$. The value of K_d^t for $R_tV_3 \cdot R'_tL'_3$ is thus estimated as $\sim 4 \times 10^{-17} \pm 1 \times 10^{-17}$ M (Eq. 3).

of V and L [making a statistical correction of a factor of 9 for the number of receptor and ligand groups in the trivalent species; $k_{on} = 9.3 \times 10^6 \text{ M}^{-1} \text{ s}^{-1}$ for V with L (21)], then k_{on} would be $\sim 8 \times 10^7 \text{ M}^{-1} \text{ s}^{-1}$, and the rate constant for dissociation of $R_tV_3 \cdot R'_tL'_3$, k_{off} , would be $k_{off} = k_{on} K_d^t \approx 3 \times 10^{-9} \text{ s}^{-1}$. Even if the association of R_tV_3 with $R'_tL'_3$ were diffusion controlled (12) and had a value of $k_{on} \approx 10^9 \text{ M}^{-1} \text{ s}^{-1}$, the estimated value of k_{off} would be $\sim 4 \times 10^{-8} \text{ s}^{-1}$. This value is compatible with our observation that the aggregate does not dissociate observably over the $>10^3$ s required for the HPLC analyses. The exchange reaction between $R_tV_3 \cdot R'_tL'_3$ and L , however, proceeded surprisingly rapidly; the reaction was nearly complete in <45 min, as evident in the HPLC traces taken during the ex-

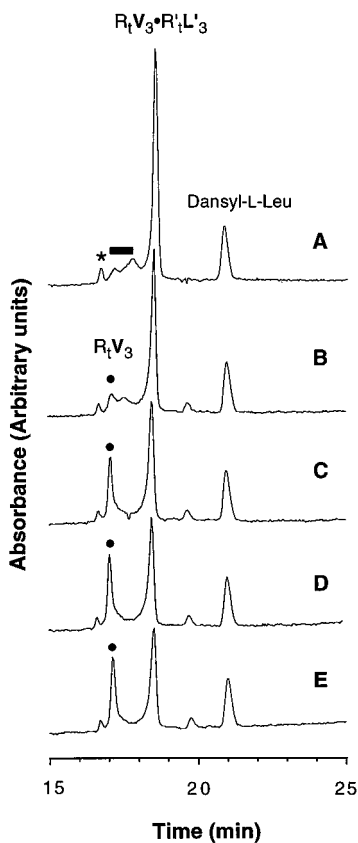


Fig. 3. Representative HPLC traces demonstrating the exchange of R_tV_3 (3 μM) + $R'_tL'_3$ (22 μM) with L (86 mM) with formation of $R_tV_3 \cdot 3L$. Exchange reactions were carried out by adding L to an equilibrated mixture of R_tV_3 and $R'_tL'_3$ and injecting it into the HPLC column after (A), 0; (B), 2; (C), 45; (D), 190; or (E), 360 min. Symbols (●) indicate the retention time of $R_tV_3 \cdot 3L$; this compound dissociates to free R_tV_3 on the column. The sample of R_tV_3 we used contained small amounts of impurities, which are indicated by the asterisk and solid bar. The conditions were similar to those in Fig. 1, except that a Vydac analytical RP column was used with the same linear gradient, run over 30 min.

change of $R_tV_3 \cdot R'_tL'_3$ with excess L (Fig. 3). Approximately 60% of the R_tV_3 remained as $R_tV_3 \cdot R'_tL'_3$ at equilibrium in a system containing L at an ~ 86 mM concentration, 17,000 times greater than the dissociation constant for the complex of R_tV_3 and L , confirming that $R_tV_3 \cdot R'_tL'_3$ was tightly associated. There is, however, an essential difference in kinetics between this trivalent system and biotin:avidin. Dissociation of $R_tV_3 \cdot R'_tL'_3$, when carried out in the presence of excess monovalent ligand L , proceeds in stages and is rapid in the presence of excess L ; dissociation of biotin:avidin necessarily proceeds to completion in one step and is slow.

We evaluated the thermodynamics of binding, using isothermal titration calorimetry (ITC) (Table 1) (25). ITC can be used to estimate K_d in the millimolar to nanomolar range. It allowed us to estimate the enthalpy of binding, ΔH° , and K_d^m for the monovalent interactions, but only ΔH° for the interaction of R_tV_3 with $R'_tL'_3$. We will analyze these complex data in detail in the future, but we note two important initial inferences from them here. First, ΔH° for the interaction between R_tV_3 and $R'_tL'_3$ is ~ -167 kJ/mol, a value that is approximately three times that for monovalent vancomycin and DADA ($\Delta H^\circ = -53.3$ kJ/mol) (13); similarly, the value of $-T\Delta S^\circ$ (where T is the temperature and ΔS° is the entropy of binding) for the trivalent species is approximately three times that of the monovalent species (26). Second, the value of K_d is remarkably indifferent to substitution on either vancomycin or L-Lys-D-Ala-D-Ala groups, so long as the interaction is monovalent; only the trivalent interaction is strong. Third, attachment of organic groups to vancomycin or L-Lys-D-Ala-D-Ala groups sometimes leads to larger values of ΔH° than is observed for unsubstituted vancomycin and diacetyl-L-Lys-D-Ala-D-Ala. We have not established the origin of this increase yet. In general, however, the data suggest that the high free energy of association of $R_tV_3 \cdot R'_tL'_3$ comes primarily from the association of three V and L groups.

The trivalent system comprising R_tV_3 and $R'_tL'_3$ is the tightest binding system in relatively low molecular weight organic species of which we know. These systems are fundamentally different from those formed by strong monovalent interactions (such as avidin:biotin), in that dissociation of the complex can be accelerated by incubation with a monovalent ligand capable of competing for the receptor sites. Avidin:biotin interactions are widely used in analytical biochemistry; we believe that tight binding systems based on polyvalency will offer alternatives and that the aspect of reversibil-

ity on addition of competing monovalent ligand will confer a degree of flexibility not possible with avidin-biotin.

REFERENCES AND NOTES

- M. N. Matrosovich, *FEBS Lett.* **252**, 1 (1989).
- A. Spaltenstein and G. M. Whitesides, *J. Am. Chem. Soc.* **113**, 686 (1991).
- Y. C. Lee and R. T. Lee, *Acc. Chem. Res.* **28**, 321 (1995).
- R. Roy and F. D. Tropper, *J. Chem. Soc. Chem. Commun.* **1988**, 1058 (1988).
- G. B. Sigal, M. Mammen, G. Dahmann, G. M. Whitesides, *J. Am. Chem. Soc.* **118**, 3789 (1996).
- Divalent interactions involving two linked ligands interacting with two linked receptors have been studied in many systems, including dimers of cyclodextrin with divalent ligands [R. Breslow and B. Zhang, *ibid.*, p. 8495], dimers of sialyl Lewis X with E-selectin [C.-H. Wong *et al.*, *ibid.* **117**, 66 (1995)], dimers of immunophilin ligands such as FK506 and cyclosporin A with receptors active in controlling cellular signal transduction [D. M. Spencer, T. J. Wandless, S. L. Schreiber, G. R. Crabtree, *Science* **262**, 1019 (1993)], and divalent antibodies with surface antigens [C. L. Hornick and F. Karush, *Immunochemistry* **9**, 325 (1972)].
- J. Rao and G. M. Whitesides, *J. Am. Chem. Soc.* **119**, 10286 (1997).
- N. M. Green, *Biochem. J.* **89**, 585 (1963).
- D. H. Williams, *Tetrahedron* **40**, 569 (1984).
- M. Schafer, T. R. Schneider, G. M. Sheldrick, *Structure* **4**, 1509 (1996).
- P. J. Loll, A. E. Bevivino, B. D. Korty, P. H. Axelsen, *J. Am. Chem. Soc.* **119**, 1516 (1997).
- D. H. Williams, *Acc. Chem. Res.* **17**, 364 (1984).
- A. Cooper and K. E. McAuley-Hecht, *Philos. Trans. R. Soc. London Ser. A* **345**, 23 (1993).
- M. Nieto and H. R. Perkins, *Biochem. J.* **123**, 773 (1971).
- P. Groves, M. S. Searle, J. P. Waltho, D. H. Williams, *J. Am. Chem. Soc.* **117**, 7958 (1995).
- U. Gerhard, J. P. Marckay, R. A. Maplestone, D. H. Williams, *ibid.* **115**, 232 (1993).
- U. N. Sundram, J. H. Griffin, T. I. Nicas, *ibid.* **118**, 13107 (1996).
- C. M. Harris and T. M. Harris, *ibid.* **104**, 4293 (1982).
- U. N. Sundram and J. H. Griffin, *J. Org. Chem.* **60**, 1102 (1995).
- The R_1V_3 hexafluoroacetate was isolated as white foam after lyophilization. The 1H -NMR spectrum showed the resonances expected for the central aromatic spacer (400 MHz, dry dimethyl- d_6 sulfoxide, δ [parts per million (ppm)] relative to tetramethylsilane (TMS): 4.45 (d, CH_2NH), 7.28 (d, ArH), 7.74 (d, ArH), 8.70 (s, ArH), 10.60 (s, CONH) and vancomycin units. The ESIMS exhibited an ion at a ratio of mass to charge (m/z) of 4818.8 consistent with the calculated molecular weight of 4815 for the parent ion ($M + H^+$), $C_{228}H_{250}N_{33}O_{72}Cl_6$. The $R'_1L'_3$ species was synthesized from coupling of N^{α} -acetyl-L-Lys-D-Ala-D-Ala-*tert*-butyl ester with 1,3,5-benzene tris (carbonyl chloride) and purified by reverse-phase HPLC after deprotection of the *tert*-butyl ester. 1H -NMR (400 MHz, dry dimethyl- d_6 sulfoxide) δ (ppm) relative to TMS: 1.16 (d, 9 H, $CHCH_3$), 1.26 (d, 9 H, $CHCH_3$), 1.22–1.36 (m, 6 H, CH_2), 1.43–1.64 (m, 12 H, CH_2), 1.81 (s, 9 H, $COCH_3$), 3.24 (d, 6 H, CH_2NH), 4.13–4.19 (m, 6 H, $COCHNH$), 4.28 (m, 3 H, $CHCH_3$), 8.03 (d, 3 H, NH), 8.08 (d, 3 H, NH), 8.15 (d, 3 H, NH), 8.34 (s, 3 H, ArH), 8.65 (t, 3 H, NH); ESIMS exhibited an ion at m/z of 1148.7 consistent with the calculated m/z of 1147 for $C_{51}H_{79}N_{12}O_{18}$ ($M + H^+$).
- The value of the rate constant for dissociation of the monovalent complex of vancomycin with **L** is $k_{off} = 31 s^{-1}$ [P. H. Popieniek and R. F. Pratt, *J. Am. Chem. Soc.* **113**, 2264 (1991)].
- A different method, ITC titration, was also used to estimate K_d^m , and yielded a slightly different value of 2.7 μM (Table 1).
- Our analyses assume that the two intermediate species, $R'_1L'_3R_1V_3 \cdot 2L$ and $R'_1L'_3R_1V_3 \cdot L$, are present in very small amounts at equilibrium and are thus negligible. This assumption leads to Eq. 5, which predicts a linear plot of $\theta/[R'_1L'_3]$ versus θ . The agreement of our experimental results with this prediction suggests that this assumption is valid under our experimental conditions.
- The values of **L**, $[R'_1L'_3]$, and θ in Eq. 5 were determined as follows: **L** was assumed to be constant, because **L** was in excess in the experiments; $[R'_1L'_3]$ was estimated from integration of the peaks for $R'_1L'_3$ on HPLC; θ was calculated using Eq. 4, where $[R_1V_3R'_1L'_3]$ was estimated from its integration, and $[R_1V_3 \cdot 3L]$ was from the integration of R_1V_3 , because $R_1V_3 \cdot 3L$ dissociated to R_1V_3 on the column (21).
- In a typical ITC experiment, a solution of the ligand is injected stepwise into a stirred solution of the receptor; after each injection, heat evolves because of binding. Integration of the evolved heats is a measure of the enthalpy of binding (ΔH°); analysis of the titration curve yields a value of the binding constant [T. Wiseman, S. Williston, J. F. Brandt, L.-N. Lin, *Anal. Biochem.* **179**, 131 (1989)].
- The entropic loss of the first binding event in the trivalent complex would be expected to be larger than that of the monovalent binding of **V** to **L**, because R_1V_3 and $R'_1L'_3$ have larger sizes and more conformational freedom than **V** and **L**. The next two steps would be less entropically unfavorable than the first binding event, because they take place intramolecularly.
- Supported by NIH grants GM 30367 (G.M.W.), GM 51559 (G.M.W.), and GM 53210 (R.M.W.). J.R. thanks Eli Lilly (1996–97) and Hoffmann-LaRoche (1997–98) for doctoral fellowships. L.I. thanks NIH for a postdoctoral fellowship.

5 January 1998; accepted 16 March 1998

An Analysis of the Origins of a Cooperative Binding Energy of Dimerization

Dudley H. Williams,* Alison J. Maguire, Wakako Tsuzuki, Martin S. Westwell

The cooperativity between binding of cell wall precursor analogs (ligands) to and antibiotic dimerization of the clinically important vancomycin group antibiotics was investigated by nuclear magnetic resonance. When dimerization was weak in the absence of a ligand, the increase in the dimerization constant in the presence of a ligand derived largely from changes associated with tightening of the dimer interface. When dimerization was strong in the absence of a ligand, the increase in the dimerization constant in the presence of a ligand derived largely from changes associated with tightening of the ligand-antibiotic interface. These results illustrate how, when a protein has a loose structure, the binding energy of another molecule to the protein can derive in part from changes occurring within the protein.

Cooperativity lies at the heart of molecular recognition, which leads to biological function (1). It is typically exercised when numerous weak interactions operate simultaneously. We may define an interaction between two molecules of A to give A·A (dimerization) as being cooperative with the binding of B to A if the equilibrium constant for the association of two molecules of B·A (to give B·A·A·B) is greater than that for $A + A \rightarrow A \cdot A$. Here, we investigate the molecular origins of such cooperativity and define a method for locating the origins of cooperative binding energy. We define the interfacial bindings in B·A and A·A as “loose” or “tight.” In tight binding, the bonds that identify the

individual interactions at the interface give a relatively large (perhaps near maximal) binding energy; that is, the average bond lengths are relatively short. In contrast, loose binding means that the corresponding interactions are associated with longer average bond lengths, which give an appreciably lower binding energy than that available in a tight structure. Loose interactions occur when the sum of the favorable bonding interactions (enthalpy) is sufficiently small to be counteracted by the adverse entropy of binding and when there is a relatively large amount of residual motion in the bound state (2).

We provide experimental evidence for the validity of the above considerations in the following sequence of steps:

1) The occurrence of loose and tight interactions, but otherwise involving a common set of weak bonds, was shown through the use of proton chemical shift changes upon association. Using the chemical shift criterion, we showed that associated structures involving one interface ($B + A \rightarrow B \cdot A$ or $A + A \rightarrow A \cdot A$) tighten at that interface as the equilibrium constant for their formation increases.

D. H. Williams, Cambridge Centre for Molecular Recognition, Department of Chemistry, University of Cambridge, Lensfield Road, Cambridge CB2 1EW, UK.
A. J. Maguire, Clinical Microbiology and Public Health Laboratory, Level 6, Addenbrookes Hospital, Hills Road, Cambridge CB2 2QW, UK.
W. Tsuzuki, National Food Research Institute, Ministry of Agriculture, Forestry and Fisheries, 2-1-2 Kannondai, Tsukuba, Ibaraki, 305 Japan.
M. S. Westwell, Dyson Perrins Laboratory, University of Oxford, South Parks Road, Oxford OX1 3QY, UK.

*To whom correspondence should be addressed. E-mail: dhw1@cam.ac.uk